Available online at www.sciencedirect.com

ScienceDirect

Current Opinion in Structural Biology

Cryo-electron microscopy analysis of myosin at work and at rest

Sean N. McMillan[1,2] and Charlotte A. Scarff[1,3]

Abstract

Myosins are a superfamily of ATP-driven actin-dependent molecular motors that are responsible for diverse functions from muscle contraction to cell division. The resolution revolution in cryo-EM has enabled characterisation of the interaction of myosin with its actin track in several states of the myosin motor cycle, for multiple myosin classes, allowing increased insight into the force generation mechanism. A major advancement in our understanding of myosin-2 regulation has come through solving structures of its shutdown state, dysregulation of which is implicated in multiple diseases. This review will discuss what has been accomplished so far with cryoEM, what is still yet to do, but within reach, and how better understanding of myosin structure–function relationships may lead to future therapeutic interventions.

Addresses

[1] The Astbury Centre for Structural Molecular Biology, University of Leeds, Leeds, LS29JT, UK

[2] School of Molecular and Cellular Biology, Faculty of Biological Sciences, University of Leeds, UK

[3] Discovery and Translational Science Department, Leeds Institute of Cardiovascular and Metabolic Medicine, School of Medicine, Faculty of Medicine & Health, University of Leeds, Leeds, LS29JT, UK

Corresponding author: Scarff, Charlotte A. (c.a.scarff@leeds.ac.uk) (Scarff C.A.)

Current Opinion in Structural Biology 2022, **75**:102391

This review comes from a themed issue on **Cryo-electron microscopy**

Edited by **Susan M. Lea** and **Pamela A. Williams**

For complete overview of the section, please refer the article collection - Cryo-electron microscopy

Available online 26 May 2022

https://doi.org/10.1016/j.sbi.2022.102391

Introduction

Myosins are a superfamily of motor proteins, comprised of at least 79 classes [1], which are responsible for movement and force generation on or along filamentous actin (F-actin) tracks fuelled by ATP hydrolysis. Myosins are comprised of a motor domain, largely conserved across all myosin classes, containing the binding sites for ATP and actin, followed by a light-chain binding domain and a tail region (Figure 1a). The motor is comprised of four subdomains, the N-terminal domain, the upper and lower 50 kDa domains (U50 and L50, respectively), and the converter domain [2]. Each of the domains are connected by loops or struts, enabling conformational flexibility in their relative positioning, which facilitates function. The converter domain and light-chain binding domain (LCD) form the lever, responsible for transmitting force, and the LCD and motor comprise the myosin head. A varied number of calmodulins or light chains (LCs) bind to the LCD. The tail region is the most varied in structure, in myosin-2, -5 and -18 containing a coiled-coil forming region that allows formation of double-headed myosin molecules, and in non-muscle myosins often contains a targeting or cargo-binding domain.

Class-2 myosins are generally responsible for muscle contraction whilst other myosins act as tethers and transporters, aiding in a broad range of functions including signal transduction, intracellular transport and cell division [3]. Whilst diverse in function, the mechanism by which myosins use the energy produced by the hydrolysis of ATP to generate force on F-actin is basically conserved (Figure 1b). Myosin is strongly-bound to F-actin in its nucleotide-free rigor state. ATP binding forces open the actin-binding cleft, weakening binding of myosin to F-actin and causing detachment. Myosin then undergoes conformational changes, during which myosin becomes primed to bind F-actin again, through a movement of the lever from a 'down' to an 'up' position, termed the recovery stroke, which is followed by ATP hydrolysis. Myosin in its ADP.Pi bound state is then able to rebind F-actin, initially weakly and then strongly, which enables phosphate release, closure of the actin-binding cleft and generation of force through swinging of the lever, termed the powerstroke [4]. Whether phosphate release precedes or follows the powerstroke is debated [5,6]. After this, further allosteric changes occur, coupled to ADP release, which enable myosins to adapt their power outputs in response to mechanical load [7]. Thus, different rates of transition between steps in the force generation cycle allow different myosin motors to be kinetically tuned for varied function. In muscle myosins, polymerisation of the tails into filaments allows for function. Muscle myosin motors spend little time attached to the actin filament as part of

Figure 1

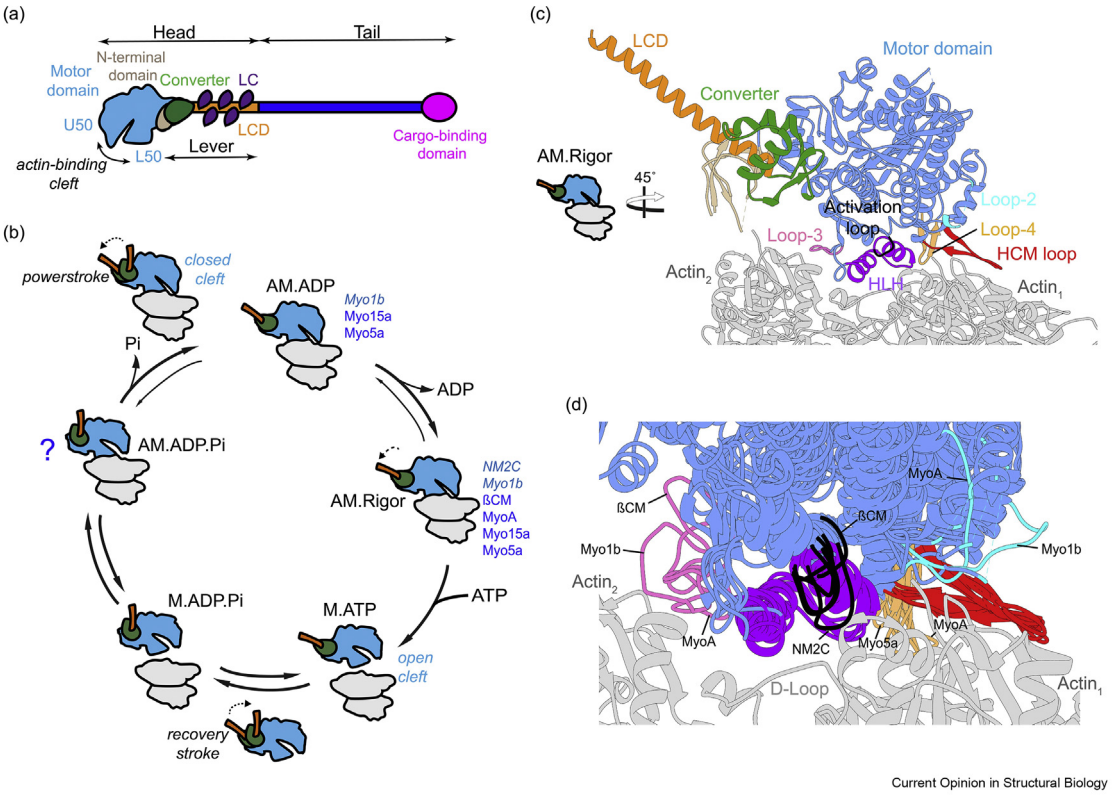

Myosin structure, the force generation cycle and strong actomyosin interface. (a) Schematic of myosin structure, consisting of a motor domain, light-chain binding domain (LCD) and tail region. The motor domain is highly conserved between myosin classes and is comprised of four sub-domains, N-terminal domain, upper (U50) and lower (L50) 50 kDa domains, and the converter, which are connected by loops and struts enabling dynamic movement. The LCD contains a varied number of binding sites for calmodulins or light chains (LC), depending on myosin class. The tail is highly variable and tuned for function. (b) Simplified schematic of the force generation cycle, highlighting myosins for which we have high resolution (3–4 Å) actomyosin structures, non-muscle myosin 2c (NM2c), myosin-1b (Myo1b), beta-cardiac myosin (βCM), *Plasmodium falciparum* myosin-A (MyoA), myosin-15a (Myo15a) and myosin-5a (Myo5a). Those solved pre-2020 are displayed in light blue whilst those solved from 2020 are shown in bright blue. AM -actomyosin, M–myosin. The structure of the primed AM.ADP.Pi state is unknown. Binding of myosin to actin induces conformational change enabling actin-binding cleft closure, phosphate release and the powerstroke. The exact order of these events is debated [5,6]. Following the powerstroke, an additional rotation of the lever arm is observed [7], highlighted by an arrow. The extent and direction of this motion is different for different myosins and affects the rate of ADP release [7] (c) Structure of rigor actomyosin (7PLU) highlighting the six elements contributing to the strongly-bound actomyosin interface, the helix-loop-helix (HLH), cardiomyopathy (HCM) loop, activation loop, loop-2, loop-3 and loop-4. Myosin binding bridges two neighbouring actin subunits labelled $Actin_1$ and $Actin_2$ (d) Comparison of the rigor actomyosin interface for non-muscle myosin-2C (NM2C; PDB ID: 5JLH), myosin-1b (Myo1b; PDB ID: 6C1H), beta-cardiac myosin (βCM; PDB ID: 7JH7), *Plasmodium falciparum* myosin-A (MyoA; PDB ID:7ALN), myosin-15a (Myo15a; PDB ID: 7R91) and myosin-5a (Myo5a; PDB ID:7PLU). The HLH and HCM loop interactions with F-actin form the core of the interface and are highly conserved. Supplementary interactions involving the activation loop, loop 2, loop 3 and loop 4 are more variable, with these regions being divergent in sequence and length. No major changes are observed in the F-actin structure upon myosin binding, though flexible regions like the D-loop become less dynamic.

their ATPase cycle (low duty ratio) and work together in assembly to move F-actin. Myosin-5 motors spend most of their ATPase cycle attached to actin (high duty ratio), enabling them to move processively along actin filaments [2,5]. Some myosins such as myosin-2, -5, -7, and -10 form autoinhibited states, which prohibit their interaction with F-actin and regulate function [8].

Mutations in myosins are implicated in many diseases, including heart disease [9], deafness [10], cancer [11,12], bleeding disorders and muscle disorders [13]. The critical roles of myosins in cellular functions and disease have led to extensive biochemical, biophysical and structural investigation, yet their dynamic nature has impeded full understanding of the force generation cycle and structure—function relationships. This is something that is now solvable with cryoEM-based technology.

Here, we describe the current contribution of cryoEM to the understanding of myosin structure and function (Table 1), with a focus on advancement over the last 2 years. We highlight the large contribution cryoEM has

Table 1

Myosin structures deposited in the Electron Microscopy Data Bank (EMDB) [16] ordered by release date, with most recent release date first. Myosin class, subtype/state, organism and nucleotide state (if known) are detailed for each structure with corresponding EMDB identifier, EM method and reported global resolution (Å), Protein Data Bank (PDB) identifier, year of deposition, and related publication reference (Ref.). TBP, to be published.

Myosin	EMDB	EM Method	Resolution (Å)	PDB	Year	Ref.
Myosin-2 smooth shutdown state (chicken)	23810	Single particle	3.4	7MF3	2021	[22]
Actomyosin-5a rigor (chicken)	13501	Helical	3.3	7PLT	2021	[19]
Actomyosin-5a rigor (chicken)	13502	Helical	3.2	7PLU	2021	[19]
Actomyosin-5a rigor (chicken)	13503	Helical	3.5	7PLV	2021	[19]
Actomyosin-5a rigor (chicken)	13504	Helical	3.5	7PLW	2021	[19]
Actomyosin-5a rigor (chicken)	13505	Helical	3.6	7PLX	2021	[19]
Actomyosin-5a rigor (chicken)	13506	Helical	3.2	7PLY	2021	[19]
Actomyosin-5a rigor (chicken)	13507	Helical	3.2	7PLZ	2021	[19]
Actomyosin-5a rigor (chicken)	13508	Helical	3.6	7PM0	2021	[19]
Actomyosin-5a rigor (chicken)	13509	Helical	3.5	7PM1	2021	[19]
Actomyosin-5a rigor (chicken)	13510	Helical	3.6	7PM2	2021	[19]
Actomyosin-5a strong-ADP (chicken)	13521	Helical	3.1	7PM5	2021	[19]
Actomyosin-5a strong-ADP (chicken)	13522	Helical	3.0	7PM6	2021	[19]
Actomyosin-5a strong-ADP (chicken)	13523	Helical	3.5	7PM7	2021	[19]
Actomyosin-5a strong-ADP (chicken)	13524	Helical	3.5	7PM8	2021	[19]
Actomyosin-5a strong-ADP (chicken)	13525	Helical	3.7	7PM9	2021	[19]
Actomyosin-5a strong-ADP (chicken)	13526	Helical	3.6	7PMA	2021	[19]
Actomyosin-5a strong-ADP (chicken)	13527	Helical	3.6	7PMB	2021	[19]
Actomyosin-5a strong-ADP (chicken)	13528	Helical	3.7	7PMC	2021	[19]
Actomyosin-5a post-rigor AppNHp (chicken)	13529	Helical	2.9	7PMD	2021	[19]
Actomyosin-5a post-rigor AppNHp (chicken)	13530	Helical	2.9	7PME	2021	[19]
Actomyosin-5a post-rigor AppNHp (chicken)	13531	Helical	3.4	7PMF	2021	[19]
Actomyosin-5a post-rigor AppNHp (chicken)	13532	Helical	3.3	7PMG	2021	[19]
Actomyosin-5a post-rigor AppNHp (chicken)	13533	Helical	3.4	7PMH	2021	[19]
Actomyosin-5a post-rigor AppNHp (chicken)	13535	Helical	3.3	7PMI	2021	[19]
Actomyosin-5a post-rigor AppNHp (chicken)	13536	Helical	3.4	7PMJ	2021	[19]
Actomyosin-5a post-rigor AppNHp (chicken)	13538	Helical	3.3	7PML	2021	[19]
Actomyosin-2 skeletal ATP (rabbit)	13328	Helical	7.5	N/A	2021	[23]
Actomyosin-15 rigor (mouse)	24322	Helical	2.8	7R91	2021	[24]
Actomyosin-15 ADP (mouse)	24399	Helical	3.6	7RB8	2021	[24]
Actomyosin-15 rigor Jordan (mouse)	24400	Helical	3.7	7RB9	2021	[24]
Actomyosin-A rigor (Plasmodium falciparum)	11818	Helical	3.7	7ALN	2021	[17]
Actomyosin-2 skeletal rigor (mouse)	12289	Subtomogram averaging	10.2	7NEP	2021	[25]
Actomyosin-2 skeletal rigor (mouse)	12291	Subtomogram averaging	15.1	N/A	2021	[25]
Myosin-2 tail (Lethocerus)	22975	Single particle	4.2	7KOG	2021	[26]
Actomyosin-A rigor (Plasmodium falciparum)	10590	Helical	3.1	6TU7	2021	TBP
Actomyosin-11 rigor (chicken)	22808	Helical	4.3	7KCH	2021	[27]
Myosin-2 smooth shutdown state (turkey)	11069	Single particle	6.3	6Z47	2020	[28]
Myosin-2 smooth shutdown state (turkey)	11070	Single particle	9.0	N/A	2020	[28]
Myosin-2 smooth shutdown state (turkey)	22145	Single particle	4.3	6XE9	2020	[29]
Actomyosin-2 cardiac rigor (pig)	22335	Helical	3.8	7JH7	2020	[20]
Myosin-2 filament (fruit fly)	22217	Single particle	7.0	N/A	2020	[30]
Myosin-2 filament mutant (fruit fly)	22218	Single particle	8.0	N/A	2020	[30]
Actomyosin-2 cardiac rigor (bovine)	22067	Helical	4.2	6X5Z	2020	[31]
Myosin-2 smooth shutdown state (turkey)	20084	Single particle	25	N/A	2019	[32]
Actomyosin-2 smooth rigor (chicken)	7100	Helical	6.0	6BIH	2019	[33]
Actomyosin-Ib ADP (rat)	7329	Helical	3.2	6C1D	2018	[7]
Actomyosin-Ib ADP (rat)	7330	Helical	3.8	6C1G	2018	[7]
Actomyosin-Ib rigor (rat)	7331	Helical	3.9	6C1H	2018	[7]
Actomyosin-6 rigor (pig)	7116	Helical	4.6	6BNP	2018	[34]
Actomyosin-6 ADP (pig)	7117	Helical	5.5	6BNQ	2018	[34]
Myosin-2 filament (Lethocerus)	7029	Single particle	6.4	N/A	2017	[35]
Actomyosin-2 skeletal rigor (rabbit)	6664	Helical	5.2	5H53	2017	[36]
Myosin-2 filament (Lethocerus)	3301	Single particle	5.5	N/A	2016	[37]
Actomyosin-10 rigor (human)	8244	Helical	9.1	5KG8	2016	[38]
Actomyosin-NM2C rigor (human)	8164	Single particle	3.9	5JLH	2016	[15]
Actomyosin-NM2C rigor (human)	8165	Single particle	3.9	5JLH	2016	[15]
Myosin-2 filament (tarantula)	6512	Single particle	13	N/A	2015	[39]
Myosin-2 filament (tarantula)	6513	Single particle	17	N/A	2015	[39]

(*continued on next page*)

Table 1 (*continued*)

Myosin	EMDB	EM Method	Resolution (Å)	PDB	Year	Ref.
Myosin-2 filament (tarantula)	6514	Single particle	30	N/A	2015	[39]
Myosin-2 filament (Schistosoma)	6370	Helical	23	3JAX	2015	[40]
Myosin-2 cardiac filament (human)	2240	Subtomogram averaging	28	N/A	2012	[41]
Myosin-2 skeletal filament (frog)	1909	Subtomogram averaging	70	N/A	2012	[42]
Actomyosin-1e rigor (slime mold)	1987	Helical	7.7	4A7F	2012	[43]
Actomyosin-1e rigor (slime mold)	1988	Helical	7.8	4A7H	2012	[43]
Actomyosin-1e rigor (slime mold)	1989	Helical	8.1	4A7L	2012	[43]
Myosin-2 smooth rigor (chicken)	5257	Electron crystallography	20	3J04	2011	[44]
Myosin-2 filament (tarantula)	1950	Helical	20	3JBH	2011	[45]
Myosin-2 cardiac filament (mouse)	1465	Helical	32	N/A	2008	[46]
Myosin-5a inhibited state (chicken)	1201	Subtomogram averaging	24	2DFS	2006	[47]
Actomyosin-2 filament (chicken)	1001	Tomography	40	1M8Q	2002	[48]
Actomyosin-2 filament (chicken)	1001	Tomography	70	1MVW	2002	[48]
Actomyosin-2 filament (chicken)	1001	Tomography	70	1O18-19	2002	[48]
Actomyosin-2 filament (chicken)	1001	Tomography	70	1O1A-F	2002	[48]

made to understanding of the force generation cycle, through providing structures of actomyosin, and in our understanding of the myosin-2 shutdown state, essential for regulation, and having significant disease relevance. We discuss what is still to find out, but obtainable by cryoEM, and how a better understanding of myosin structure–function relationships may lead to future therapeutic interventions.

Myosin dynamics and the actomyosin cycle

The myosin motor has been extensively characterised by X-ray crystallography in a range of nucleotide and mutational states to provide a detailed picture of the conformational changes myosin undergoes when not interacting with actin [2,5]. However, X-ray crystallography cannot capture the details of how myosin interacts with its track, F-actin, in actomyosin states of the force generation cycle. These states have been studied by electron microscopy since the 1970s [14] but only recent improvements in cryoEM instrumentation and image processing have enabled high-resolution (3–4 Å) actomyosin structure determination, first achieved in 2016 [15]. Over the past 6 years, the number of cryoEM actomyosin structures available has increased rapidly (Table 1), providing a picture of the entire force generation cycle (Figure 1b), with only the initial binding of myosin, in its primed state, to actin left to elucidate [4]. In the past two years alone, the number of high-resolution (3–4 Å) actomyosin structures deposited in the electron microscopy databank (EMDB) [16] has increased from five to 32 (Table 1). In addition, a number of medium resolution structures have been deposited and interpreted with the aid of existing crystal structures. This has consolidated our knowledge of the actomyosin rigor and strong-ADP states, enabling increased understanding of conserved features of the actomyosin interface across myosin species and those that are specific to particular myosins and thus relatable to certain functional and/or kinetic properties.

A comparison of the available actomyosin rigor and strong-ADP bound high-resolution structures shows that six elements contribute to the actomyosin interaction surface in these states (Figure 1c,d). The helix-loop-helix (HLH) and cardiomyopathy (HCM) loop interactions form the core of the interface [17] and this is largely conserved. Small differences in supplementary actomyosin interactions involving loop-2, loop-3, the activation loop, and loop-4, are related to differences in loop sequence and length, which adapt them for function. Loop-2 is involved in initial sensing of the actin-binding interface and likely modulates weak-binding of myosin in its primed state to F-actin [18]. Loop-3 is generally longer, and makes more extensive interactions with F-actin, in high-duty ratio motors (e.g. myosin-1b, myosin-5 and myosin-6) [7,19], whilst there is no interaction between loop-3 and F-actin for the low-duty ratio beta-cardiac myosin [20]. The activation loop is involved in binding F-actin for some myosins and not others. The variable position of loop-4 may influence a binding preference for F-actin with or without tropomyosin [5]. The actin-binding cleft is closed in all structures and there are no major changes in F-actin upon myosin binding, although some flexible regions like the D-loop become less dynamic. The transition between strong-ADP and rigor states does not affect the actomyosin interface but is associated with conformational change within the motor domain, which, relieves internal strain, facilitates nucleotide release, and results in small movement of the lever [21].

Despite the core of the actomyosin interface being conserved, small conformational changes are propagated through the motor domains resulting in large differences in the relative positions of the converter and LCD for the different myosin classes. Recently, multiple structures of myosin-5 have illustrated heterogeneity in the lever position within three nucleotide states [19]. The dynamic nature of the different actomyosin states

means that the structure of each class of myosin molecule in each step of the force generation cycle needs to be elucidated in order to understand the nuances of the process for each myosin in detail. One large gap in our understanding of the force generation cycle comes from the lack of any actomyosin structures in the primed state that would describe how myosin initially attaches to F-actin. This is something that is likely to be imminently addressed through the use of time-resolved cryoEM. Pioneering work showed disordered binding of single-headed myosin to F-actin occurred before formation of the classic actomyosin-rigor complex [49], suggesting that it was possible to trap transient intermediates. Recent advances in time-resolved cryoEM grid preparation devices have enabled reproducible rapid mixing and grid vitrification on millisecond timescales [23] and modern microscopes should enable these transient structures to be determined to high-resolution.

Myosin tails

Whilst high-resolution structures of myosin heads have been determined, information regarding the structures of myosin tails is sparse. Assembly of myosin-2 into filaments is essential for function, with correct tail packing needed to ensure the appropriate arrangement of heads on the thick filament backbone. Thick filaments have only been solved to medium resolutions (5–8 Å) for invertebrates [30,37,39] and low resolution (20–30 Å) for vertebrates [41,46]. This has increased our understanding of tail packing for invertebrate filaments and has led to a structure of the full-length myosin-2 tail, by extracting segments of density relating to a single tail from a thick filament reconstruction [26]. The tail adopts a canonical coiled coil throughout its length except at the head–tail junction and around skip residues, which interrupt the characteristic heptad repeat synonymous with coiled coil. The tail is seen to flex along the filament backbone and undergo local unwinding of the super-helical repeat. There is remarkable agreement between this invertebrate tail structure and the 13 available crystals structures of human myosin tail segments, which together cover just less than half of the coiled-coil length, except in the tail region immediately following the head (proximal S2), and around skip residues 2 and 4 [26].

Myosin regulation

An exciting new area of muscle biology is the discovery of new mechanisms of myosin thick filament regulation, and the involvement of this regulation in disease, discussed in detail elsewhere [50–54] and outlined here. In myosin-2, a conserved structural regulatory state termed the interacting-heads motif (IHM) has been observed in both filaments and isolated myosin molecules [55]. In the IHM [56], the two motor domains of the same myosin molecule interact asymmetrically with one another, creating one head that is blocked (BH) from interacting with F-actin by occlusion of its actin-binding site, and one head termed free (FH) (Figure 2a). Both heads are in a primed conformation and are thought to have low basal ATPase activity [53]. In relaxed striated muscle, myosin heads are found in the IHM state along the thick filament backbone, interacting with the first section of their own coiled-coil tail and with adjacent heads [46] (Figure 2b). The sequestering of heads away from F-actin together with low basal ATPase activity underlies vertebrate thick-filament based regulation of contraction [50] and the so-called super-relaxed state [54]. In smooth muscle and non-muscle cells, regulatory light chain (RLC) dephosphorylation can promote depolymerisation of myosin filaments [57], and individual myosin molecules can form the shutdown state. In this state, the heads adopt the IHM with the tail wrapped around the heads, bent into three segments (Figure 2c) [58]. This shutdown state may facilitate transport of myosin within the cytoplasm.

High-resolution structures of relaxed thick filaments and shutdown myosin molecules have the potential to aid in understanding of myosin-2 regulation and to reveal how dysregulation of the IHM may underlie multiple human diseases. Unfortunately, thick filament structures have been of insufficient resolution to achieve this. The difficulties in thick filament isolation and their dynamic nature limits resolution rather than the cryoEM imaging technique. Recently, in seminal work by Wang et al. [25], the potential for in situ determination of myosin structures has been shown through a sub-nm reconstruction of actomyosin by subtomogram averaging and this approach may well result in high-resolution thick filament reconstructions in the future. The shutdown state, observed in smooth muscle and non-muscle myosin-2, is significantly more stable than the IHM observed in striated muscle myosin, due to the presence of additional stabilising interactions between the tail and heads, and has been successfully captured by single-particle approaches.

Three shutdown smooth muscle myosin (SmM) cryoEM structures have been solved in the last 2 years [22,28,29]. Not surprisingly, all three corresponding PDB models are extremely similar in the heads region, where the cryoEM density maps are highly consistent and model building is aided by the availability of crystal structures. Each of the PDB models describe the same main interfaces that stabilise the shutdown state (Figure 2d) and propose a similar regulatory mechanism for its destabilisation upon RLC phosphorylation (Figure 2e). The phosphorylation sites are found in the N-terminal extensions of the RLCs, which form the latch (BH RLC – tail segment 3 interactions) and mortar (RLC–RLC) interactions within the shutdown state respectively. Phosphorylation disrupts these

Figure 2

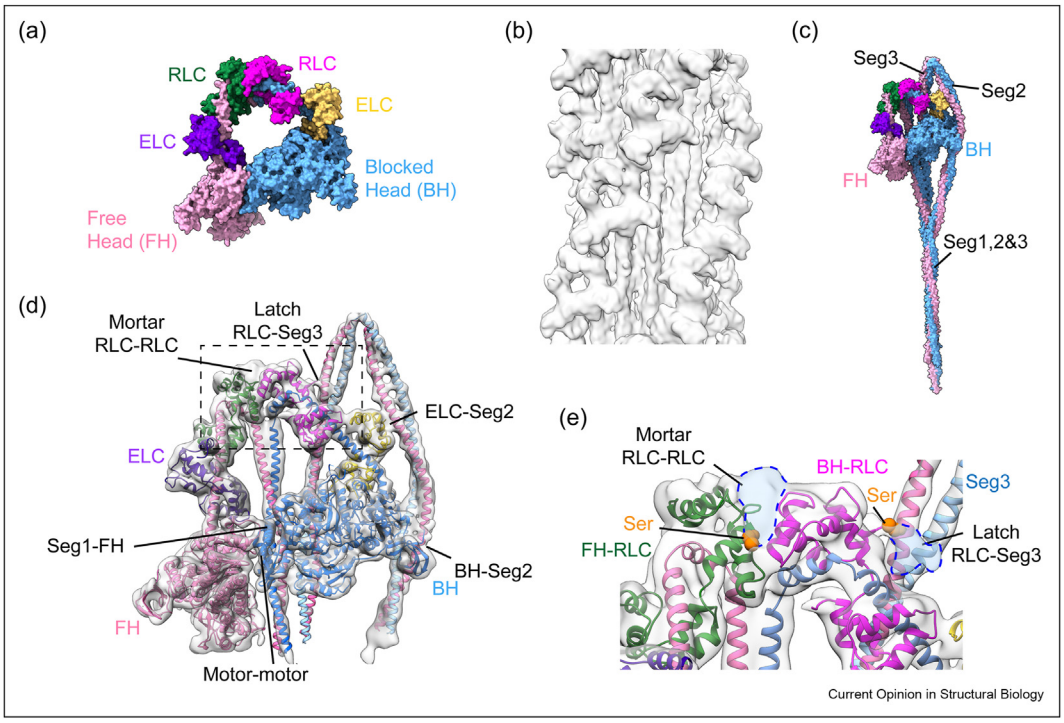

The Interacting-heads motif and shutdown state of myosin-2. (a) Schematic of the interacting-heads motif (IHM). One head is blocked (BH) from interacting with F-actin by binding to the converter domain of the free head (FH), RLC - regulatory light chain, ELC – essential light chain (b) Observation of the IHM in cryoEM reconstruction of tarantula thick filaments (EMDB ID:6512) [39](c) Space-filled model of the shutdown state of smooth muscle myosin (SmM), showing the blocked head – BH, free head-FH, and the relative positions of the three tail segments, seg1, seg2 and seg3 (d) PDB ID: 6Z47 inset into EMDB cryoEM density map:11069 [28], illustrating interactions between the motor domains, light chains and tail segments within the heads region of the SmM shutdown state. (e) Enlarged view of (d) (boxed region) in latch and mortar regions, showing location of phosphorylatable serine residues (orange) and unfilled density attributable to N-terminal extensions of the RLCs (shaded pale blue and outlined with dashed blue line). The structure suggests the mechanism of regulation by phosphorylation. Phosphorylation of the BH-RLC serine (orange) would cause charge repulsion between the latch and segment 3, whilst phosphorylation of the FH-RLC serine (orange) would cause steric clashes pushing apart mortar interactions to open the molecule up.

interactions by creating charge repulsion in the latch and steric clashes in the mortar, releasing the tail from the BH and pushing apart the head–tail junction so that the molecule can open up. However, there are inconsistences between the PDB structures for the tail, specifically for tail segments 2 and 3. This is not surprising given their inherent flexibility, demonstrated by differences here in the overlay of the maps, and lower resolution in the experimental data within this region prohibiting *de novo* building. The Scarff et al. [28] structure is of lower global resolution (6.3 Å) but was obtained from an unfixed, native molecule, whilst the other structures (3.4–4.3 Å) were stabilised by cross-linking [22,29]. Scarff et al. [28] used constraints from coiled-coil geometry to ensure canonical coiled coils were built into the lower resolution tail density, whilst Yang et al. [29] and Heissler et al. [22] did not. These latter models contain significant regions of tail which lack the hydrophobic seam associated with a canonical coiled coil.

Structure-based drug design

Obtaining more structures at high-resolution to reveal structural–functional relationships, brings strong potential for structure-based drug design in the myosin field. In particular, over 1000 mutations in the beta-cardiac myosin molecule are associated with cardiomyopathies [13], with significant disease burden. These mutations are spread throughout the molecule, with hotspots around the nucleotide pocket, converter and segment-1 region of the tail [13]. Although some mutations modulate force generation, or actomyosin interactions [20,59], many are suggested to affect formation or stabilisation of the IHM [59,60]. Small molecule modulators of cardiac myosin are already in clinical trials for cardiomyopathies [61–64] and one of these, mavacamten, is known to stabilise an off-state [65]. The recently solved shutdown state of myosin-2 provides a framework for interpreting the effects of mutation on structure. A high-resolution structure of the beta-cardiac myosin IHM, and of the shutdown state

of non-muscle myosin 2A, which is dysregulated in clotting disorders, would be targets for structure-based drug design. The malaria parasite myosin seems significantly divergent in structure–function relationships from human myosins that it could be a target for malaria treatment [17,66]. Class I myosins are implicated in cancer and could prove potential targets for diagnostic, prognostic, and therapeutic purposes in the future [11].

Conclusions

CryoEM is revolutionising the myosin field, providing actomyosin structures to reveal a more complete understanding of the force generation cycle, and structures of autoinhibited states, with potential for structure-based drug design. It is highly likely that time-resolved cryoEM will soon enable the primed actomyosin state to be solved to high-resolution. Single-particle approaches to solve autoinhibited states of myosin will surely continue. Vertebrate myosin filaments have so far eluded high-resolution structure determination, largely because of difficulties in their purification as well as inherent dynamics. Further improvements in cryo-electron tomography and its increased implementation in the myosin/muscle arena may allow for determination of myosin filament structures to high-resolution in situ.

Author contributions

Charlotte A. Scarff: Writing - Review & Editing, Data Curation, Visualization. Sean M. McMillian: Writing - Review & Editing, Data Curation, Validation.

Conflict of interest statement

Nothing declared.

Acknowledgements

We thank Prof. Michelle Peckham, Prof. Peter Knight, Dr. Glenn Carrington and Dr. David Casas-Mao for critical reading of the manuscript. This work was supported by a British Heart Foundation Jacqueline Murray Coomber Fellowship (FS/20/21/34704) to C.S and a School of Molecular and Cellular Biology, Faculty of Biological Sciences, University of Leeds, funded PhD studentship to S.M.

References

Papers of particular interest, published within the period of review, have been highlighted as:

- • of special interest
- •• of outstanding interest

1. Kollmar M, Mühlhausen S: **Myosin repertoire expansion coincides with eukaryotic diversification in the Mesoproterozoic era**. *BMC Evol Biol* 2017, **17**:211.

2. Sweeney HL, Houdusse A, Robert-Paganin J: **Myosin structures BT - myosins: A superfamily of molecular motors**. In *Myosins, advances in experimental medicine and biology*. Edited by Coluccio LM, Springer International Publishing; 2020:7–19.

3. Sweeney HL, Holzbaur ELF: **Motor proteins**. *Cold Spring Harbor Perspect Biol* 2018, **10**.

4. Schröder RR: **The structure of acto-myosin BT - myosins: A superfamily of molecular motors**. In *Myosins, advances in experimental medicine and biology*. Edited by Coluccio LM, Springer International Publishing; 2020:41–59.

5. •• Robert-Paganin J, Pylypenko O, Kikuti C, Sweeney HL, Houdusse A: **Force generation by myosin motors: a structural perspective**. *Chem Rev* 2020, **120**:5–35.
Exceptional review highlighting what we currently know about force generation by myosin motors

6. • Debold EP: **Recent insights into the relative timing of myosin's powerstroke and release of phosphate**. *Cytoskeleton* 2021, **78**:448–458.
Insightful review examining the evidence for phosphate release preceding or following the powerstroke

7. Mentes A, Huehn A, Liu X, Zwolak A, Dominguez R, Shuman H, Ostap EM, Sindelar CV: **High-resolution cryo-EM structures of actin-bound myosin states reveal the mechanism of myosin force sensing**. *Proc Natl Acad Sci Unit States Am* 2018, **115**:1292–1297.

8. Heissler SM, Sellers JR: **Various themes of myosin regulation**. *J Mol Biol* 2016, **428**:1927–1946.

9. Barrick SK, Greenberg MJ: **Cardiac myosin contraction and mechanotransduction in health and disease**. *J Biol Chem* 2021, **297**:101297.

10. Cirilo JA, Gunther LK, Yengo CM: **Functional role of class III myosins in hair cells**. *Front Cell Dev Biol* 2021, **9**.

11. Diaz-Valencia JD, Estrada-Abreo LA, Rodríguez-Cruz L, Salgado-Aguayo AR, Patiño-López G: **Class I Myosins, molecular motors involved in cell migration and cancer**. *Cell Adhes Migrat* 2022, **16**:1–12.

12. Peckham M: **How myosin organization of the actin cytoskeleton contributes to the cancer phenotype**. *Biochem Soc Trans* 2016, **44**:1026–1034.

13. Parker F, Peckham M: **Disease mutations in striated muscle myosins**. *Biophys Rev* 2020, **12**:887–894.

14. Moore PB, Huxley HE, DeRosier DJ: **Three-dimensional reconstruction of F-actin, thin filaments and decorated thin filaments**. *J Mol Biol* 1970, **50**:279–292.

15. von der Ecken J, Heissler SM, Pathan-Chhatbar S, Manstein DJ, Raunser S: **Cryo-EM structure of a human cytoplasmic actomyosin complex at near-atomic resolution**. *Nature* 2016, **534**:724–728.

16. Lawson CL, Patwardhan A, Baker ML, Hryc C, Garcia ES, Hudson BP, Lagerstedt I, Ludtke SJ, Pintilie G, Sala R, *et al.*: **EMDataBank unified data resource for 3DEM**. *Nucleic Acids Res* 2016, **44**:D396–D403.

17. • Robert-Paganin J, Xu X-P, Swift MF, Auguin D, Robblee JP, Lu H, Fagnant PM, Krementsova EB, Trybus KM, Houdusse A, *et al.*: **The actomyosin interface contains an evolutionary conserved core and an ancillary interface involved in specificity**. *Nat Commun* 2021, **12**:1892.
Details of the actomyosin interface and its conserved core

18. Yengo CM, Sweeney HL: **Functional role of loop 2 in myosin V**. *Biochemistry* 2004, **43**:2605–2612.

19. •• Pospich S, Sweeney HL, Houdusse A, Raunser S: **High-resolution structures of the actomyosin-V complex in three nucleotide states provide insights into the force generation mechanism**. *Elife* 2021, **10**.
Actomyosin-V in three nucleotide states to high-resolution illustrating conformational flexibility

20. • Risi C, Schäfer LU, Belknap B, Pepper I, White HD, Schröder GF, Galkin VE: **High-resolution cryo-EM structure of the cardiac actomyosin complex**. *Structure* 2021, **29**:50–60. e4.
Details of the cardiac actomyosin complex and the impact of disease mutations on the interface

21. Wulf SF, Ropars V, Fujita-Becker S, Oster M, Hofhaus G, Trabuco LG, Pylypenko O, Sweeney HL, Houdusse AM, Schröder RR: **Force-producing ADP state of myosin bound to actin**. *Proc Natl Acad Sci Unit States Am* 2016, **113**:E1844–E1852.

22. •• Heissler SM, Arora AS, Billington N, Sellers JR, Chinthalapudi K: **Cryo-EM structure of the autoinhibited state of myosin-2**. *Sci Adv* 2022, **7**:eabk3273.
Most recent cryoEM structure of shutdown state of myosin-2 obtained to high resolution

23. Klebl DP, White HD, Sobott F, Muench SP: **On-grid and in-flow mixing for time-resolved cryo-EM**. *Acta Crystallogr D* 2021, **77**: 1233–1240.

24. • Gong R, Jiang F, Moreland ZG, Reynolds MJ, Espinosa de los Reyes S, Gurel PS, Shams A, Bowl MR, Bird JE, Alushin GM: *Structural basis for tunable control of actin dynamics by myosin-15 in mechanosensory stereocilia*. bioRxiv; 2021, https://doi.org/10.1101/2021.07.09.451843.
CryoEM of actomyosin-15 in multiple states illustrating how myosin-15 may regulate actin

25. •• Wang Z, Grange M, Wagner T, Kho AL, Gautel M, Raunser S: **The molecular basis for sarcomere organization in vertebrate skeletal muscle**. *Cell* 2021, **184**:2135–2150. e13.
Seminal work using cryoET and subtomogram averaging to reveal actomyosin structures in situ

26. •• Rahmani H, Ma W, Hu Z, Daneshparvar N, Taylor DW, McCammon JA, Irving TC, Edwards RJ, Taylor KA: **The myosin II coiled-coil domain atomic structure in its native environment**. *Proc Natl Acad Sci Unit States Am* 2021, **118**, e2024151118.
First structure of a full-length myosin-2 tail determined by cryoEM

27. Ruijgrok PV, Ghosh RP, Zemsky S, Nakamura M, Gong R, Ning L, Chen R, Vachharajani VT, Chu AE, Anand N, *et al.*: **Optical control of fast and processive engineered myosins in vitro and in living cells**. *Nat Chem Biol* 2021, **17**:540–548.

28. •• Scarff CA, Carrington G, Casas-Mao D, Chalovich JM, Knight PJ, Ranson NA, Peckham M: **Structure of the shutdown state of myosin-2**. *Nature* 2020, **588**:515–520.
One of two initial structures of the shutdown state of myosin-2, describing key interactions interfaces

29. •• Yang S, Tiwari P, Lee KH, Sato O, Ikebe M, Padrón R, Craig R: **Cryo-EM structure of the inhibited (10S) form of myosin II**. *Nature* 2020, **588**:521–525.
One of two initial structures of the shutdown state of myosin-2, describing key interactions interfaces

30. Daneshparvar N, Taylor DW, O'Leary TS, Rahmani H, Abbasiyeganeh F, Previs MJ, Taylor KA: **CryoEM structure of Drosophila flight muscle thick filaments at 7 Å resolution**. *Life Sci Alliance* 2020, **3**:e202000823.

31. Doran MH, Pavadai E, Rynkiewicz MJ, Walklate J, Bullitt E, Moore JR, Regnier M, Geeves MA, Lehman W: **Cryo-EM and molecular docking shows myosin loop 4 contacts actin and tropomyosin on thin filaments**. *Biophys J* 2020, **119**:821–830.

32. Yang S, Lee KH, Woodhead JL, Sato O, Ikebe M, Craig R: **The central role of the tail in switching off 10S myosin II activity**. *J Gen Physiol* 2019, **151**:1081–1093.

33. Banerjee C, Hu Z, Huang Z, Warrington JA, Taylor DW, Trybus KM, Lowey S, Taylor KA: **The structure of the actin-smooth muscle myosin motor domain complex in the rigor state**. *J Struct Biol* 2017, **200**:325–333.

34. Gurel PS, Kim LY, Ruijgrok PV, Omabegho T, Bryant Z, Alushin GM: **Cryo-EM structures reveal specialization at the myosin VI-actin interface and a mechanism of force sensitivity**. *Elife* 2017, **6**:e31125.

35. Hu Z, Taylor DW, Edwards RJ, Taylor KA: **Coupling between myosin head conformation and the thick filament backbone structure**. *J Struct Biol* 2017, **200**:334–342.

36. Fujii T, Namba K: **Structure of actomyosin rigour complex at 5.2 Å resolution and insights into the ATPase cycle mechanism**. *Nat Commun* 2017, **8**:13969.

37. Hu Z, Taylor DW, Reedy MK, Edwards RJ, Taylor KA: **Structure of myosin filaments from relaxed Lethocerus flight muscle by cryo-EM at 6 Å resolution**. *Sci Adv* 2016, **2**:e1600058.

38. Ropars V, Yang Z, Isabet T, Blanc F, Zhou K, Lin T, Liu X, Hissier P, Samazan F, Amigues B, *et al.*: **The myosin X motor is optimized for movement on actin bundles**. *Nat Commun* 2016, **7**: 12456.

39. Yang S, Woodhead JL, Zhao F-Q, Sulbarán G, Craig R: **An approach to improve the resolution of helical filaments with a large axial rise and flexible subunits**. *J Struct Biol* 2016, **193**: 45–54.

40. Sulbarán G, Alamo L, Pinto A, Márquez G, Méndez F, Padrón R, Craig R: **An invertebrate smooth muscle with striated muscle myosin filaments**. *Proc Natl Acad Sci Unit States Am* 2015, **112**: E5660–E5668.

41. AL-Khayat HA, Kensler RW, Squire JM, Marston SB, Morris EP: **Atomic model of the human cardiac muscle myosin filament**. *Proc Natl Acad Sci Unit States Am* 2013, **110**:318–323.

42. Luther PK, Winkler H, Taylor K, Zoghbi ME, Craig R, Padrón R, Squire JM, Liu J: **Direct visualization of myosin-binding protein C bridging myosin and actin filaments in intact muscle**. *Proc Natl Acad Sci Unit States Am* 2011, **108**:11423–11428.

43. Behrmann E, Müller M, Penczek PA, Mannherz HG, Manstein DJ, Raunser S: **Structure of the rigor actin-tropomyosin-myosin complex**. *Cell* 2012, **150**:327–338.

44. Baumann BAJ, Taylor DW, Huang Z, Tama F, Fagnant PM, Trybus KM, Taylor KA: **Phosphorylated smooth muscle heavy meromyosin shows an open conformation linked to activation**. *J Mol Biol* 2012, **415**:274–287.

45. Brito R, Alamo L, Lundberg U, Guerrero JR, Pinto A, Sulbarán G, Gawinowicz MA, Craig R, Padrón R: **A molecular model of phosphorylation-based activation and potentiation of tarantula muscle thick filaments**. *J Mol Biol* 2011, **414**: 44–61.

46. Zoghbi ME, Woodhead JL, Moss RL, Craig R: **Three-dimensional structure of vertebrate cardiac muscle myosin filaments**. *Proc Natl Acad Sci Unit States Am* 2008, **105**:2386–2390.

47. Liu J, Taylor DW, Krementsova EB, Trybus KM, Taylor KA: **Three-dimensional structure of the myosin V inhibited state by cryoelectron tomography**. *Nature* 2006, **442**:208–211.

48. Chen LF, Blanc E, Chapman MS, Taylor KA: **Real Space refinement of acto-myosin structures from sectioned muscle**. *J Struct Biol* 2001, **133**:221–232.

49. Walker M, Zhang XZ, Jiang W, Trinick J, White HD: **Observation of transient disorder during myosin subfragment-1 binding to actin by stopped-flow fluorescence and millisecond time resolution electron cryomicroscopy: evidence that the start of the crossbridge power stroke in muscle has variable geometry**. *Proc Natl Acad Sci U S A* 1999, **96**:465–470.

50. Irving M: **Regulation of contraction by the thick filaments in skeletal muscle**. *Biophys J* 2017, **113**:2579–2594.

51. Elisabetta B, Luca F, Andrea G, So-Jin P-H, OJ G, Theyencheri N, Malcolm I: **Myosin filament-based regulation of the dynamics of contraction in heart muscle**. *Proc Natl Acad Sci Unit States Am* 2020, **117**:8177–8186.

52. Hill C, Brunello E, Fusi L, Ovejero JG, Irving M: **Myosin-based regulation of twitch and tetanic contractions in mammalian skeletal muscle**. *Elife* 2021, **10**:e68211.

53. Spudich JA: **Three perspectives on the molecular basis of hypercontractility caused by hypertrophic cardiomyopathy mutations**. *Pflügers Arch - Eur J Physiol* 2019, **471**:701–717.

54. McNamara JW, Li A, Dos Remedios CG, Cooke R: **The role of super-relaxed myosin in skeletal and cardiac muscle**. *Biophys Rev* 2015, **7**:5–14.

55. Lee KH, Sulbarán G, Yang S, Mun JY, Alamo L, Pinto A, Sato O, Ikebe M, Liu X, Korn ED, *et al.*: **Interacting-heads motif has been conserved as a mechanism of myosin II inhibition since before the origin of animals**. *Proc Natl Acad Sci Unit States Am* 2018, **115**:E1991–E2000.

56. Wendt T, Taylor D, Trybus KM, Taylor K: **Three-dimensional image reconstruction of dephosphorylated smooth muscle heavy meromyosin reveals asymmetry in the interaction between myosin heads and placement of subfragment 2**. *Proc Natl Acad Sci Unit States Am* 2001, **98**:4361–4366.

57. Wang L, Chitano P, Seow CY: **Filament evanescence of myosin II and smooth muscle function**. *J Gen Physiol* 2021, **153**: e202012781.

58. Burgess SA, Yu S, Walker ML, Hawkins RJ, Chalovich JM, Knight PJ: **Structures of smooth muscle myosin and heavy**

meromyosin in the folded, shutdown state. *J Mol Biol* 2007, **372**:1165–1178.

59. Trivedi DV, Adhikari AS, Sarkar SS, Ruppel KM, Spudich JA: **Hypertrophic cardiomyopathy and the myosin mesa: viewing an old disease in a new light**. *Biophys Rev* 2018, **10**:27–48.

60. Alamo L, Ware JS, Pinto A, Gillilan RE, Seidman JG, Seidman CE, Padrón R: **Effects of myosin variants on interacting-heads motif explain distinct hypertrophic and dilated cardiomyopathy phenotypes**. *Elife* 2017, **6**, e24634.

61. Teerlink JR, Diaz R, Felker GM, McMurray JJV, Metra M, Solomon SD, Adams KF, Anand I, Arias-Mendoza A, Biering-Sørensen T, *et al.*: **Cardiac myosin activation with omecamtiv mecarbil in systolic heart failure**. *N Engl J Med* 2020, **384**: 105–116.

62. Biering-Sørensen T, Minamisawa M, Liu J, Claggett B, Papolos AI, Felker GM, McMurray JJV, Legg JC, Malik FI, Honarpour N, *et al.*: **The effect of the cardiac myosin activator, omecamtiv mecarbil, on right ventricular structure and function in chronic systolic heart failure (COSMIC-HF)**. *Eur J Heart Fail* 2021, **23**:1052–1056.

63. Olivotto I, Oreziak A, Barriales-Villa R, Abraham TP, Masri A, Garcia-Pavia P, Saberi S, Lakdawala NK, Wheeler MT, Owens A, *et al.*: **Mavacamten for treatment of symptomatic obstructive hypertrophic cardiomyopathy (EXPLORER-HCM): a randomised, double-blind, placebo-controlled, phase 3 trial**. *Lancet* 2020, **396**:759–769.

64. Alsulami K, Marston S: **Small molecules acting on myofilaments as treatments for heart and skeletal muscle diseases**. *Int J Mol Sci* 2020, **21**:9599.

65. Anderson RL, Trivedi DV, Sarkar SS, Henze M, Ma W, Gong H, Rogers CS, Gorham JM, Wong FL, Morck MM, *et al.*: **Deciphering the super relaxed state of human β-cardiac myosin and the mode of action of mavacamten from myosin molecules to muscle fibers**. *Proc Natl Acad Sci Unit States Am* 2018, **115**:E8143–E8152.

66. • Moussaoui D, Robblee JP, Auguin D, Krementsova EB, Haase S, Blake TCA, Baum J, Robert-Paganin J, Trybus KM, Houdusse A: **Full-length Plasmodium falciparum myosin A and essential light chain PfELC structures provide new anti-malarial targets**. *Elife* 2020, **9**:e60581.
Structures of *Plasmodium falciparum* myosin A and their potential use as anti-malaria targets.